MULTIAXIAL DAMAGE IDENTIFICATION OF ANGLE-PLY LAMINATES USING ACOUSTIC EMISSION AND OTHER ONLINE MONITORING TECHNIQUES

Kalliopi-Artemi Kalteremidou[1], Eleni Tsangouri[1], Anghel Cernescu[1,2], Brendan R. Murray[1,2], Lincy Pyl[1], Dimitrios G. Aggelis[1] and Danny Van Hemelrijck[1]

[1]Department of Mechanics of Materials and Constructions, Vrije Universiteit Brussel (VUB),
Pleinlaan 2, BE-1050 Brussels, Belgium
Email: Kalliopi-Artemi.Kalteremidou@vub.be, Eleni.Tsangouri@vub.be,
Anghel-Vasile.Cernescu@vub.be, Brendan.Murray@vub.be, Lincy.Pyl@vub.be,
Dimitrios.Aggelis@vub.be, Danny.Van.Hemelrijck@vub.be
Web Page: http://www.vub.ac.be/MEMC/
[2]SIM M3 Program, Technologiepark 935, B-9052 Zwijnaarde, Belgium
Web Page: http://www.sim-flanders.be/research-program/m3

Keywords: carbon fiber reinforced composites, non destructive techniques, acoustic emission, damage investigation, multiaxiality

Abstract

The aim of this research is the combined use of acoustic emission with other online monitoring techniques in order to identify the damage sequence of carbon fiber reinforced epoxies. Initially, common lay-ups were tested and their acoustic emission was monitored and analyzed with respect to the developing damage, in order to identify basic damage modes. Following this, angle-ply laminates were tested to characterize the damage evolution under multiaxial stress states with the use of acoustic emission and supporting techniques.

1. Introduction

In service, composite materials are often subjected to multiaxial stresses. Damage of composites is not as straightforward as in the case of more conventional materials especially under multiaxial loads. However, the influence of multiaxiality on their static and dynamic mechanical behavior still remains an open and dominant question. In literature, it is shown that the combination of transverse and shear stresses is detrimental, especially under fatigue [1]. Therefore, it is crucial to understand, to characterize, and to create predictive tools for the influence of multiaxiality on the damage process and the mechanical response of the composite material being analyzed.

One of the most promising Non Destructive Techniques (NDTs) used for the detection of early stage damage and for the characterization of different damage modes under service loads is Acoustic Emission (AE). AE allows the detection and analysis of elastic waves that originate in the material due to different

damage mechanisms. Therefore, initially AE can be used as a predictive tool for failure based on the detection of early stage damage and, moreover, it allows the identification of the occurring stress states and the damage mechanisms developed in a material. In literature, research on the AE damage identification of composite materials has been conducted but no direct correlation to multiaxial stress states has been performed [2-4].

In order to study the influence of multiaxiality in composites, different geometric configurations can be used. For example, external multiaxiality can be applied in tubular specimens under tension/torsion or in cruciform ones loaded biaxially. On the contrary, internal multiaxiality can be studied in flat laminates under uniaxial tension, since any change in the laminate lay-up can introduce different multiaxial stresses at the lamina level [5]. As shown in literature, the investigation of the impact of internal multiaxial stress states on flat laminates has lead to significant conclusions regarding the influence of external multiaxial stresses on complex geometries [6]. Additionally, manufacturing of non-unidirectional tubular specimens and testing of cruciform specimens is still not straightforward, whereas testing of standard coupons is much easier and better established.

For all the above reasons, in this study, different Carbon Fiber Reinforced Polymer (CFRP) flat specimens were tested under static tensile loads. Common lay-ups at which the damage process is more straightforward were initially tested. After this, angle-ply laminates with different lay-ups were subjected to static loads, in order to study the effects of the different multiaxiality they experienced. AE was applied in all tests in order to identify the damage process and the AE signals related to specific damage modes. Optical methods accompanied the AE findings, with an optical microscope capturing the through-the-thickness damage, along with Digital Image Correlation (DIC) which measured the full-field strain distributions.

This research is a first step towards the full comprehension of damage of composites under different stresses. The results shown here refer only to quasi-static loads but a full understanding of these findings can lead to the characterization and identification of damage in more realistic fatigue loads.

2. Materials and equipment

In this study, CFRP laminates consisting of carbon fibers and epoxy resin, manufactured by Mitsubishi Chemical Corporation, were used. First, in a simplified scenario, common CFRP lay-ups ($[0^o]_4$, $[90^o]_8$, $[0^o/90^o]_{2s}$ and $[45^o/-45^o]_{2s}$) were tested under static tension conditions. Emitted AE signals were classified based on AE feature analysis in order to identify dominant damage modes (matrix cracking, fiber failure, etc.). The results were used for the study of multiaxial stress fields and for this analysis two angle-ply laminates were used: $[0^o/30^o]_{2s}$ and $[0^o/60^o]_{2s}$. Their mechanical behavior was analyzed with respect to the biaxiality ratios (i.e. $\lambda_{12}=\sigma_6/\sigma_2$, where σ_2 is the transverse stress and σ_6 is the in-plane stress in the material coordinates system) that are developed in the off-axis layers.

Specimens were cut with dimensions according to ASTM D3039 and all of them were tabbed for a length of 50 mm on both sides using the same CFRP material with a $[45^o/-45^o]_{2s}$ lay-up. All tests were performed on a MTS servo-hydraulic machine with a load cell of 100 kN capacity. The static tests were performed in displacement control with a rate of 1 mm/min. At least 3 repetitions for each case were performed.

In order to monitor the acoustic activity during testing, an eight-channel DiSP system by Mistras Group was used. Two piezoelectric transducers (Pico) with a broadband response and maximum sensitivity at 450 kHz were mounted on the specimen using vaseline. The signals were amplified using preamplifiers with a uniform gain of 40 dB and a 35 dB threshold was applied in order to filter out the noise of the mechanical system [3]. Before testing, lead break tests were performed in order to check the sensitivity of the transducers and to calculate the surface wave speed.

Kalliopi-Artemi Kalteremidou, Eleni Tsangouri, Anghel Cernescu, Brendan R. Murray, Lincy Pyl, Dimitrios G. Aggelis and Danny Van Hemelrijck

The deflection during testing was measured using a 50 mm extensometer. At the same time, a DIC system (VIC-3D by Correlated Solutions with two Stingray Cameras of 5 MP and 23 mm lenses) was used in order to obtain the full-field strain maps during testing through triangulation of the two cameras. Moreover, a Leica microscope was mounted on the frame of the MTS system. This allowed for the monitoring of the through-thickness damage of the material in specific steps during testing.

The combination of the above mentioned NDTs was used in order to understand the damage process of the CFRP laminates for the different lay-ups and to characterize their AE response.

3. Results and discussion

In order to obtain the mechanical properties of the CFRP material under investigation, standard tests on $[0^o]_4$, $[90^o]_8$ and $[45^o/-45^o]_{2s}$ specimens were initially performed. In Table 1, the measured material properties are presented.

Table 1. Elastic and strength properties of the CFRP material.

Engineering constant	Unit	Value
$\sigma_{1,U}$	[MPa]	2272.43
$\sigma_{2,U}$	[MPa]	55.00
$\sigma_{6,U}$	[MPa]	52.27
E_1	[GPa]	125.83
E_2	[GPa]	9.40
G_{12}	[GPa]	4.06

These lay-ups were also used to characterize their AE response with respect to their damage sequence. After the identification of their overall AE activity, a preliminary feature analysis based on events obtained from linear location algorithms was performed. Based on this, a preliminary separation of the obtained events in groups was performed and correlation of these groups with the expected damage mechanisms was done. The first important remark is that for all lay-ups, a specific group of signals was recorded for the whole test, characterized by small wave risetime (delay between the onset and the maximum peak) and amplitude (voltage of the maximum peak). These signals can be attributed to preliminary micro-damage manifestation, system noise not successfully removed, reverberation phenomena or minor friction events. As these signals are not clearly identified, they will be named as group 0 signals.

Beginning with the $[0^o]_4$ laminates, the curves in Figure 1 show the evolution of the stress together with the increase in the cumulative AE events during the static loading. As it is clearly shown, limited AE is recorded for the initial half of the test. Only after an applied stress of 950 MPa is achieved, an increase in the AE events occurs, consisting of group 0 signals, as well as signals with higher risetime and amplitude. These signals increase in population as the test progresses and have a mean risetime value of 53.5 µs and an amplitude of 83.6 dB. These AE events can be attributed to fiber breaks and will be referred as group 1 signals. A sudden increase of these signals takes place at an applied stress of 1850 MPa, which corresponds to small continuous load drops, acting as indicators for the occurrence of multiple fiber breaks. The basic damage mode appearing in this lay-up is fiber breaks, which can also be

Kalliopi-Artemi Kalteremidou, Eleni Tsangouri, Anghel Cernescu, Brendan R. Murray, Lincy Pyl, Dimitrios G. Aggelis and Danny Van Hemelrijck

shown by the microscope, with which visible fiber breaks were shown at a stress equal to 85% of the ultimate. After a stress of 2100 MPa is achieved, signals with much higher risetime (mean value of 145.7 μs) but similar amplitude also occur, which is presumed to be related to fiber pull-out and interlaminar delaminations, prior to the ultimate failure of the material (group 2 signals).

In Figure 2, the corresponding response for a [90º]$_8$ laminate is plotted. Similar to the previous case, almost no AE is monitored for the initial half of the test and then an increase in the events is recorded until the failure of the material. However, the difference in the total number of events is noticeable, since limited matrix micro-cracks are the main damage mode in this specific configuration, leading therefore to an almost linear stress increase without any load drops and with no visible damage by the microscope. The [90º]$_8$ laminates are characterized by the appearance of signals with a mean risetime value of 78.2 μs and a median amplitude of 49.6 dB. These signals are attributed to matrix micro-cracks of low intensity, which are not able to propagate in the material.
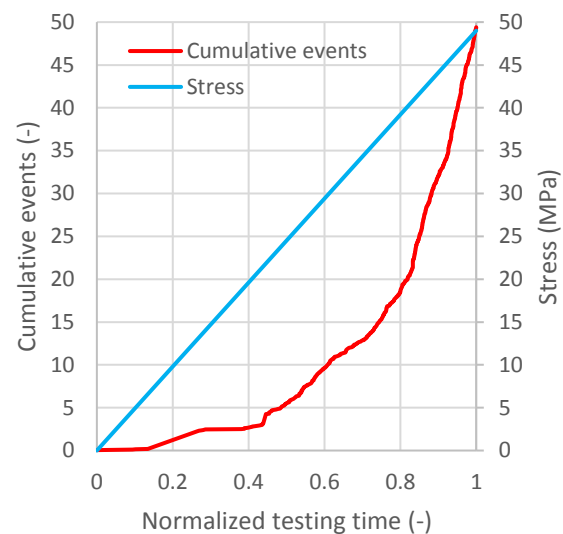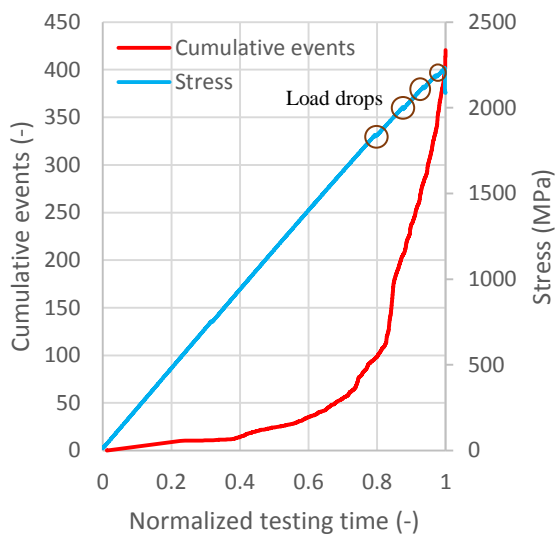
Figure 1. Increase of cumulative events and stress for a [0º]$_4$ laminate.

Figure 2. Increase of cumulative events and stress for a [90º]$_8$ laminate.

In Figure 3, the corresponding response of a [0º/90º]$_{2s}$ laminate is shown. In this laminate, matrix cracks are expected to occur quite earlier than other damage modes since the 90º layers fail earlier than the 0º ones. Later, delaminations and fiber breaks, which lead to the final failure of the material, are expected. In contrast with the previous laminates, in this case, monitoring of damage with the online microscope during the test is more helpful. From such monitoring, it was found that visible cracks occur at a stress of around 400 MPa, while AE shows very limited activity until a stress level of 300 MPa, and after this it increases rapidly. In this case, the signals recorded after a stress of 300 MPa have similar risetime as the signals of the [90º]$_8$ laminates attributed to matrix cracks, with the only difference that they are characterized by a higher average amplitude (73.4 dB). Since they correspond not only to micro cracks, but also to bigger cracks visible with the microscope which are able to propagate and to generate more events of higher energy, these signals are related to matrix cracks and will be referred to as group 3. As the test proceeds, these group 3 signals related to matrix cracks start saturating, leading to a reduction in the slope of the events and give rise to signals similar to groups 1 and 2 related to fiber breaks and interlaminar delaminations towards the end of the test, with the online microscopy confirming the appearance of delaminations in the last 10-15% of the remaining load (above a stress of 1100 MPa).

Kalliopi-Artemi Kalteremidou, Eleni Tsangouri, Anghel Cernescu, Brendan R. Murray, Lincy Pyl, Dimitrios G. Aggelis and Danny Van Hemelrijck

As the last case of the common laminate configurations, in Figure 4, the corresponding response of a $[45°/-45°]_{2s}$ laminate is plotted. In this case, the main damage is attributed to shear stresses and the main observation was that this laminate leads to very high number of events in relation to its ultimate stress. Events start to occur after a stress of 50 MPa is applied and then they continue increasing exponentially. These signals are attributed to intralaminar shear debondings and shear friction. In this case, the signals have an increasing high risetime with a mean value of 127.2 µs, but are characterized by small amplitudes of 54.8 dB (group 4). At a stress value equal to 100 MPa, interlaminar delamination was observed with the microscope which corresponds to the appearance of group 2 signals, and after that a load drop was recorded corresponding to the development of shear cracks visible with the DIC.
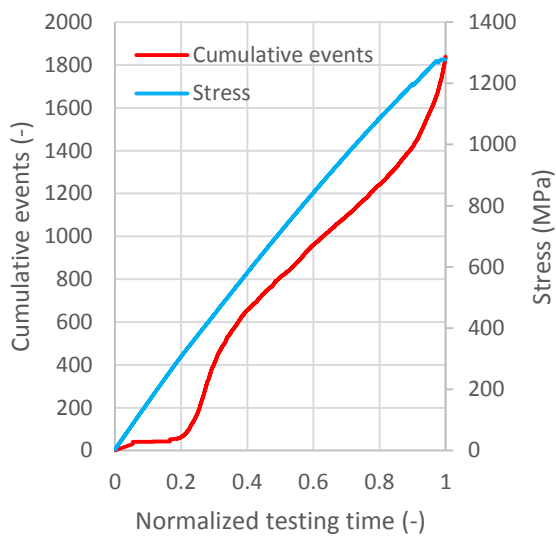
Figure 3. Increase of cumulative events and stress for a $[0°/90°]_{2s}$ laminate.
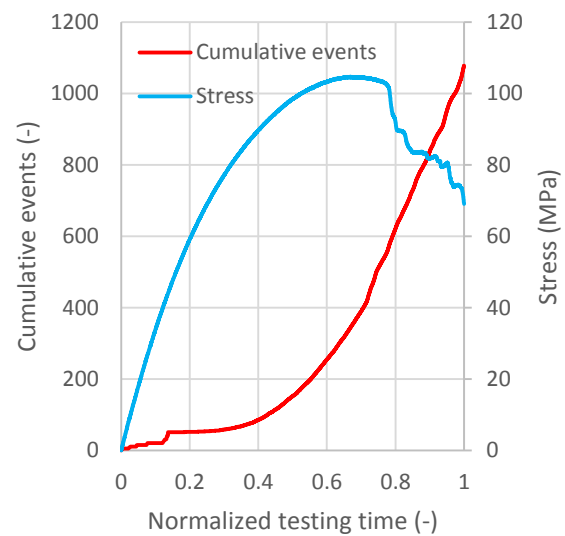
Figure 4. Increase of cumulative events and stress for a $[45°/-45°]_{2s}$ laminate.

A characteristic example of the different types of signals appearing in a $[0°/90°]_{2s}$ laminate is shown in Figure 5, in which the evolution of the risetime throughout the test is plotted. The standard deviation is quite high due to the stochastic nature of the phenomena, however, the transition of the centers of the different groups is indicative of the different damage modes.
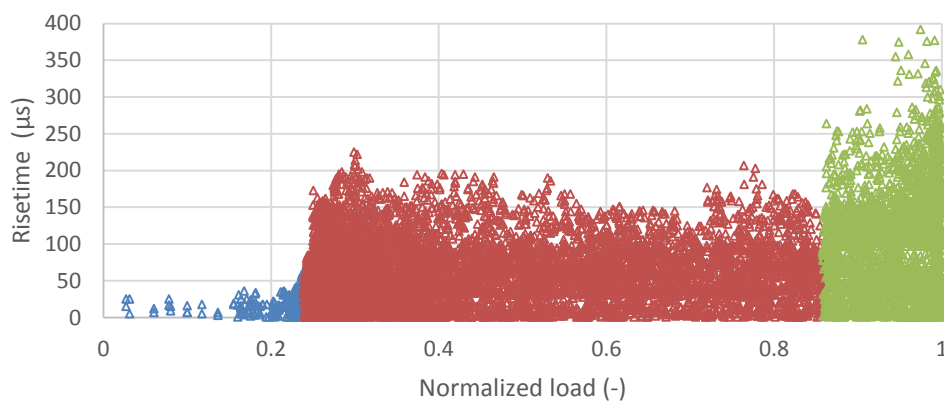
Figure 5. Evolution of risetime for a $[0°/90°]_{2s}$ laminate.

Kalliopi-Artemi Kalteremidou, Eleni Tsangouri, Anghel Cernescu, Brendan R. Murray, Lincy Pyl, Dimitrios G. Aggelis and Danny Van Hemelrijck

As a further step, two angle-ply laminates, $[0^o/30^o]_{2s}$ and $[0^o/60^o]_{2s}$, were tested. In Table 2, the mechanical properties of the two angle-ply laminates, namely $[0^o/30^o]_{2s}$ and $[0^o/60^o]_{2s}$, are shown. Looking at Table 2, it is worth mentioning that both laminates present similar mechanical behavior. The $[0^o/30^o]_{2s}$ laminates result in a 4.1% gain in ultimate strength and a 5.2% gain in stiffness compared to the $[0^o/60^o]_{2s}$ laminates due to the fibers in their off-axis layers which are less inclined with respect to the loading direction than in the $[0^o/60^o]_{2s}$ laminates.

Table 2. Mechanical properties of the off-axis laminates measured from the quasi-static tests.

	Ultimate strength [MPa]	E-modulus [GPa]	Strain to failure [%]
$[0^o/30^o]_{2s}$	1374.57	78.15	1.57
$[0^o/60^o]_{2s}$	1317.53	74.11	1.71

However, the two laminates underwent distinctly different damage processes. Concerning the $[0^o/30^o]_{2s}$ laminates, until 70% of the ultimate load, no damage was observed and after a splitting of the fibers on the outer 0° layer, at around 75% load an initial delamination between this 0° and the adjacent 30° layer was evident. At this stage, only some limited matrix cracks were recorded in the middle thick 30° layer. Between 75% and 85% of the load (Figure 6), the second outer 0° layer also delaminated from its adjacent 30° layer. At 85% load, multiple cracks on one of the thin 30° layers were recorded and a third delamination between this and the inner 0° layer was visible. For the $[0^o/60^o]_{2s}$ laminates, even from a load equal to 45% of the ultimate one, matrix cracks in all 60° layers were observed. Until 85% load, an increase in the matrix crack density was observed (Figure 6) and only at a load level corresponding to 90% of the ultimate load was an initial delamination between the outer 0° layer and the adjacent 60° layer recorded which led to the final failure. The above observations can be explained and correlated with the stress states acting on the lamina level of the two lay-ups. In the $[0^o/30^o]_{2s}$ laminates, the λ_{12} ratio is equal to 2.02 while in the $[0^o/60^o]_{2s}$ laminates it is equal to 0.64, showing that the $[0^o/30^o]_{2s}$ laminates are subject to local intralaminar shear debondings which lead to interlaminar delaminations, whereas in the $[0^o/60^o]_{2s}$ specimens the matrix cracks are more pronounced.

(a)

(b)
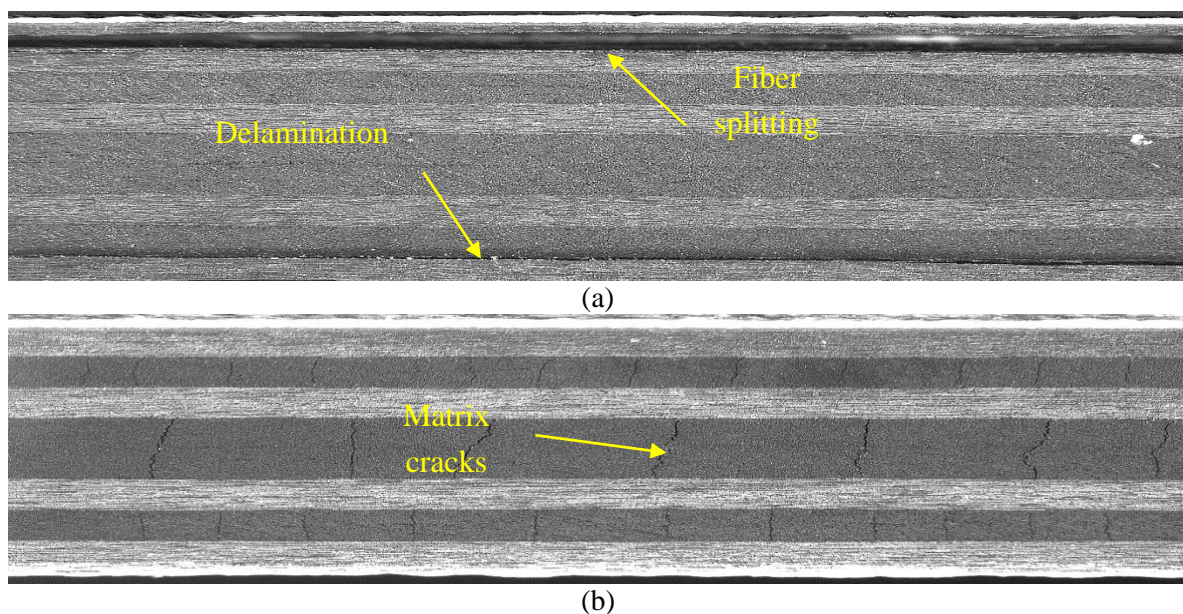
Figure 6. Damaged state at 75% load for (a) $[0^o/30^o]_{2s}$ laminates and (b) $[0^o/60^o]_{2s}$ laminates.

Kalliopi-Artemi Kalteremidou, Eleni Tsangouri, Anghel Cernescu, Brendan R. Murray, Lincy Pyl, Dimitrios G. Aggelis and Danny Van Hemelrijck

In Figure 7, the total AE for the two laminates is shown and the findings here present a good correlation with the previous results. The first remark is that for the $[0º/30º]_{2s}$ laminates, more AE events are recorded in comparison to the $[0º/60º]_{2s}$ ones. Moreover, only the $[0º/30º]_{2s}$ laminates exhibit an exponential increase in AE events. For the $[0º/60º]_{2s}$ laminates, limited AE activity is observed below 400 MPa, and beyond this point, AE events with the same features as group 3 signals are recorded (which are related to initial matrix microcracking). The same signals are recorded at a stress level of 600 MPa, which coincides with the stage at which matrix cracks were observed with the microscope. These signals increase in population during the test and are the dominant signals measured, confirming their correspondence to matrix cracks. This is also in good agreement with the increase of matrix cracks during the test as observed with the microscope. As the stress increases, the appearance of group 4 signals slowly occurs, corresponding to intralaminar shear debondings due to the increase of the shear stress in the 60º layers. The increase of the events continues until a 90% stress and after this a sudden increase in the AE events is observed, coinciding with the appearance of interlaminar delaminations in the microscopy images, which is confirmed by the rise of group 2 signals. On the other hand, the $[0º/30º]_{2s}$ laminates show AE activity earlier than the $[0º/60º]_{2s}$ laminates even if no damage is monitored. Most of this activity can be attributed to local intralaminar shear debondings quite early in the test which increase exponentially until the final failure. This hypothesis is confirmed with the appearance of group 4 signals of high risetime and low amplitude from the beginning until the end of the test. An increase in the AE activity is recorded after a stress of 1000 MPa, when the first visible damage occurs and intralaminar shear debondings lead to interlaminar delaminations. This is also confirmed by the appearance of group 2 signals at a stress level below 1000 MPa, much earlier than the appearance of these signals for the $[0º/60º]_{2s}$ laminates.
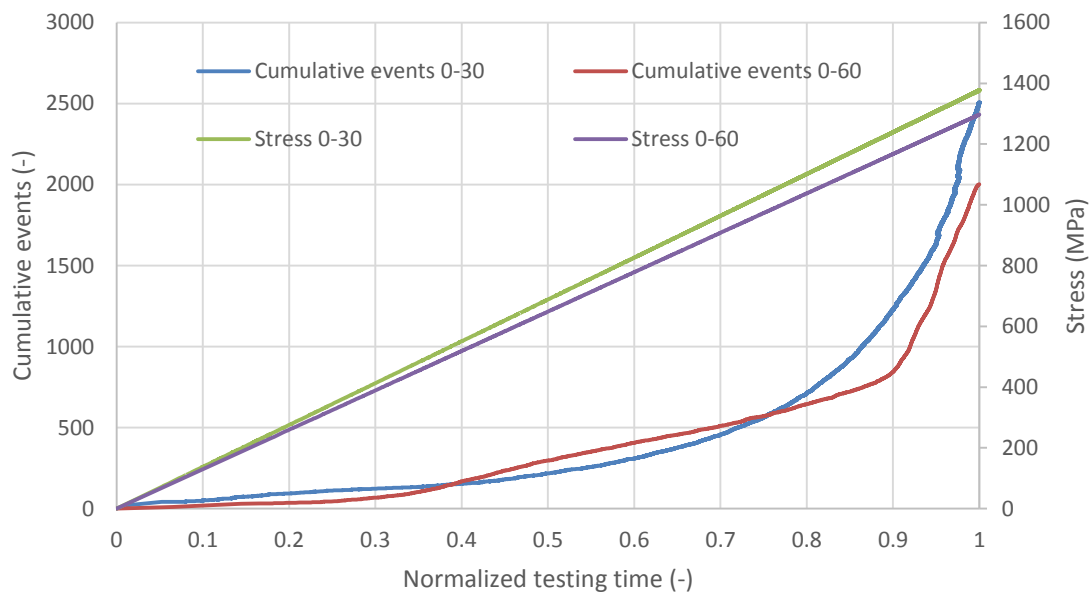
Figure 7. Increase of cumulative events and stress for the angle-ply laminates.

4. Conclusions

In the current work, identification of damage modes in CFRPs by means of acoustic emission and online microscopy was studied. Common lay-ups were tested in order to characterize the AE signals attributed to specific damage modes. In a second step, the influence of the different multiaxial stress states and, more significantly, the influence of the shear component on the static behavior of two angle-ply

Kalliopi-Artemi Kalteremidou, Eleni Tsangouri, Anghel Cernescu, Brendan R. Murray, Lincy Pyl, Dimitrios G. Aggelis and Danny Van Hemelrijck

laminates was examined. Under static loads, the shear influence was not shown in the mechanical response but it influenced the damage progress. Higher shear components have shown a greater possibility for the appearance of intralaminar shear debondings which lead to the initiation of interlaminar delaminations. This was confirmed by the AE findings, since signals related to shear debondings were the dominant ones for the $[0^o/30^o]_{2s}$ laminates, while signals related to matrix cracks appeared with a higher population early in the test for the $[0^o/60^o]_{2s}$. These signals were then saturated following the saturation of matrix cracks, and gave rise to signals related to shear debondings, when a specific shear stress was achieved. Therefore, the identification of multiaxial stress states and resulting damage modes in CFRPs was shown to be possible with acoustic emission techniques.

Acknowledgments

References

[1]   A.S. Chen and F.L. Matthews. A review of multiaxial/biaxial loading tests for composite materials. *Composites Journal,* 24:395–406, 1993.

[2]   D.G. Aggelis, N.M. Barkoula, T.E. Matikas, and S.A. Paipetis. Acoustic emission monitoring of degradation of cross ply laminates. *Journal of the Acoustical Society of America*, 127:246-251, 2010.

[3]   N. Godin, S. Huguet, R. Gaertner, and L. Salmon. Clustering of acoustic emission signals collected during tensile tests on unidirectional glass/polyester composite using supervised and unsupervised classifiers. *NDT E International Journal*, 37:253–264, 2004.

[4]   V. Kostopoulos, T.H. Loutas, A. Kontsos, G. Sotiriadis, and Y.Z. Pappas. On the identification of the failure mechanisms in oxide/oxide composites using acoustic emission. *NDT E International Journal*, 36:571–580, 2003.

[5]   K.A. Kalteremidou, S. Fonteyn, D. Carrella-Payan, L. Pyl, and D. Van Hemelrijck. Experimental investigation of the fatigue behaviour of off-axis CFRP laminates using Non Destructive Techniques. *Proceedings of the 21st International Conference on Composite Materials ICCM-21, Xi'an, China*, August 20-25 2017.

[6]   M. Quaresimin and L. Susmel. Multiaxial fatigue behaviour of composite laminates. *Key Engineering Materials Journal*, 221–222: 71–80, 2002.

Kalliopi-Artemi Kalteremidou, Eleni Tsangouri, Anghel Cernescu, Brendan R. Murray, Lincy Pyl, Dimitrios G. Aggelis and Danny Van Hemelrijck